Journal of Biomechanics 96 (2019) 109327

Contents lists available at ScienceDirect

Journal of Biomechanics

journal homepage: www.elsevier.com/locate/jbiomech
www.JBiomech.com

A probabilistic method to estimate gait kinetics in the absence of ground reaction force measurements

Kevin Tanghe [a,*], Maarten Afschrift [b], Ilse Jonkers [b], Friedl De Groote [b], Joris De Schutter [a], Erwin Aertbeliën [a]

[a] Robotics Research Group[1], Department of Mechanical Engineering, KU Leuven, 3001 Heverlee, Belgium
[b] Human Movement Biomechanics Research Group, Department of Movement Sciences, KU Leuven, 3001 Heverlee, Belgium

ARTICLE INFO

Article history:
Accepted 30 August 2019

Keywords:
Joint torques
Ground reaction forces and moments
Estimation
Inverse Dynamics
Gait

ABSTRACT

Human joint torques during gait are usually computed using inverse dynamics. This method requires a skeletal model, kinematics and measured ground reaction forces and moments (GRFM). Measuring GRFM is however only possible in a controlled environment. This paper introduces a probabilistic method based on probabilistic principal component analysis to estimate the joint torques for healthy gait without measured GRFM. A gait dataset of 23 subjects was obtained containing kinematics, measured GRFM and joint torques from inverse dynamics in order to obtain a probabilistic model. This model was then used to estimate the joint torques of other subjects without measured GRFM. Only kinematics, a skeletal model and timing of gait events are needed. Estimation only takes 0.28 ms per time instant. Using cross-validation, the resulting root mean square estimation errors for the lower-limb joint torques are found to be approximately 0.1 Nm/kg, which is 6–18% of the range of the ground truth joint torques. Estimated joint torque and GRFM errors are up to two times smaller than model-based state-of-the-art methods. Model-free artificial neural networks can achieve lower errors than our method, but are less repeatable, do not contain uncertainty information on the estimates and are difficult to use in situations which are not in the learning set. In contrast, our method performs well in a new situation where the walking speed is higher than in the learning dataset. The method can for example be used to estimate the kinetics during overground walking without force plates, during treadmill walking without (separate) force plates and during ambulatory measurements.

1. Introduction

Gait analysis (Gage, 1993) is often used for clinical decision making, selecting effective patient treatment and gaining insight in the loading of the musculoskeletal system. State-of-the-art gait analysis systems combine an optical motion capture system for kinematic data with multi-axial force plates (Chambers and Sutherland, 2002; Simon, 2004). The joint torques are usually estimated using these measurements in an inverse dynamics method (Winter, 1987). However, force plates are expensive, complicate the measurements since they require that each foot lands on a force plate, and can only be used in a laboratory environment.

Some researchers therefore developed hardware alternatives to force plates. Instrumented shoes (Schepers et al., 2007; Zheng et al., 2008) are again expensive and prone to overloading, while pressure insoles (Chumanov et al., 2010; Khurelbaatar et al., 2015) can only measure the vertical force component and need an extensive calibration procedure. Others developed methods to estimate GRFM from measured kinematics and contact information, i.e. whether or not a foot is in contact with the ground. For example, the GRFM can be estimated based on the distance of the feet to the center of pressure (Davis and Cavanagh, 1993) or the zero moment point (Dijkstra and Gutierrez-Farewik, 2015). However, these methods do not allow the computation of all components of the GRFM. Another possibility is to use foot-ground contact models to estimate the full GRFM. Contact models use visco-elastic force elements (Jackson et al., 2016; Jung et al., 2014; Lugrís et al., 2013) or muscle-like force elements (Fluit et al., 2014). To obtain a high accuracy, the parameters of these models are often subject-specific and need to be identified from measured GRFM. After this identification, the contact model can estimate the GRFM using only kinematic data. Another way to estimate the full GRFM is to use the smooth transition assumption (Ren et al., 2008) where GRFM values during the double support phase are determined based on the last value in the single support phase and an empirical transition function. Similar studies (Samadi

[1] The Robotics Research Group is a University Core Lab of Flanders Make.

* Corresponding author.
E-mail address: kevin.tanghe@kuleuven.be (K. Tanghe).

https://doi.org/10.1016/j.jbiomech.2019.109327
0021-9290/

et al., 2017; Shahabpoor and Pavic, 2018) determined other empirical transition functions, but did not estimate all the components of the GRFM. These methods need a dataset of walking experiments of different subjects to learn a general transition function and the accuracy depends on the similarity between the general transition function and the true transition function of the subject. Another possibility to estimate GRFM are artificial neural networks (Oh et al., 2013), learned from a large training dataset containing kinematics and kinetics. After learning, the neural network can accurately predict the kinetics using only kinematic measurements.

All of the above methods first estimate the GRFM and then use inverse dynamics to estimate the joint torques. In this way, estimation errors of the GRFM accumulate in the computation of the joint torques. In contrast, we introduce a probabilistic method that uses measured kinematics and contact information to estimate the joint torques and the GRFM simultaneously.

2. Methods

2.1. Gait dataset

A dataset of 23 healthy young subjects (age 21 ± 2, 14 female and 9 male) walking on a treadmill was collected. The ethics committees of UZ KU Leuven and the School of Healthcare Sciences of Cardiff University approved the experimental protocol. Participants provided written, informed consent prior to participating. We analyzed 1 min of walking at 4 km/h for all 23 subjects after 5 min of adaptation to the treadmill. For 7 out of the 23 subjects, we additionally analyzed walking at 3 and 5 km/h. In total, 934 steps (not equally distributed over the different participants) were observed. A generic musculoskeletal model with 37 degrees of freedom (Hamner et al., 2010; OpenSim, 2009) was extended with a degree of freedom for knee adduction and scaled to the anthropometry of the subject using the standard method of OpenSim (Delp et al., 2007). Vicon cameras (Vicon, Oxford) measured the trajectories of 48 retroreflective markers in an extended plug-in gait marker protocol (Davis et al., 1991) at a frequency of 100 Hz. Joint kinematics were calculated from the 3D marker coordinates using a Kalman smoothing algorithm (De Groote et al., 2008). An instrumented, dual split-belt treadmill (Grail, MotekMedical) recorded the GRFM under each foot separately at a frequency of 1000 Hz. A forth-order low-pass Butterworth smoother with a cut-off frequency of 8 Hz was applied to the GRFM. The smoothed GRFM were expressed as a 3D force and a 3D moment acting on the calcaneus of each foot. The timing of the initial contact (IC) and toe off (TO) was determined from the GRFM: IC occurs when the vertical force exceeds 20 N; TO occurs when the vertical force drops below 20 N. Inverse dynamics was applied to calculate the ground truth values of the joint torques.

2.2. Method

The dynamic equations of a skeletal model can be used to estimate the joint torques and GRFM. However, this set of equations is underdetermined during double support, resulting in an infinite number of solutions. During single support, the dynamic equations have a unique solution, but this solution is sensitive to inaccuracies in the skeletal model (Fluit et al., 2014). In this work, a probabilistic model of joint torques and GRFM is used to overcome the indeterminacy and to reduce the sensitivity to skeletal model inaccuracies.

Fig. 1 shows the method outline. In the learning phase, gait kinematics and GRFM of different subjects are measured and used to calculate joint torques using inverse dynamics. From this dataset, a model of the joint torques and GRFM is learned. This model is probabilistic, it deals with model and measurement uncertainty in a Bayesian way. It contains latent variables $\mathbf{x}^*$ that cannot be measured directly but have to be inferred indirectly. These latent variables do not have fixed values, but are described by a probability distribution. In the estimation phase, the learned model is used to estimate the latent variables, the joint torques and GRFM of a new subject, using only measured kinematics, a skeletal model of the subject, and the timing of IC (initial contact) and TO (toe off) of each foot. This is realized by maximizing the likelihood of the estimated joint torques and GRFM given the learned probabilistic model and the available measurements. This approach results in joint torques and GRFM that are as consistent as possible with the current measurements and observations of the dataset.

2.2.1. Learning phase

In the learning phase, a probabilistic model of the lower-limb joint torques and GRFM of a complete gait cycle is learned from a dataset. A gait cycle is described by a normalized time s which is zero at IC of a foot, and increases linearly with time until it is equal to one at the next IC of the same foot. For each leg, hip extension, hip adduction, hip rotation, knee flexion, knee adduction, ankle flexion and the six components of the GRFM are modeled as a function of s. The joint torques $\boldsymbol{\tau}$ and GRFM $\boldsymbol{\lambda}$ are scaled with a diagonal matrix $\mathbf{S}$, containing the body mass as diagonal elements, to obtain the scaled joint torques $\tilde{\boldsymbol{\tau}}$ and scaled GRFM $\tilde{\boldsymbol{\lambda}}$:

$$\begin{bmatrix} \tilde{\boldsymbol{\tau}}(s) \\ \tilde{\boldsymbol{\lambda}}(s) \end{bmatrix} = \mathbf{S}^{-1} \begin{bmatrix} \boldsymbol{\tau}(s) \\ \boldsymbol{\lambda}(s) \end{bmatrix} \tag{1}$$

Due to the scaling, the learned model can be used for subjects with a large difference in body mass.

A probabilistic model for the scaled signals is formed inspired by Aertbeliën and De Schutter (2014). For each recorded gait cycle i, the six scaled joint torques and six GRFM of each leg are interpolated at d normalized time steps $s_1, s_2, \ldots, s_d$ with $s_1 = 0$ at the start and $s_d = 1$ at the end of the gait cycle, resulting in row vectors $\tilde{\tau}_j^i(s_1, \ldots, s_d)$ and $\tilde{\lambda}_j^i(s_1, \ldots, s_d)$, with $j = 1 \ldots 6$, which are collected in the i-th row of matrix $\mathbf{Y}$:

$$\begin{aligned} \mathbf{Y}(i,:) = \; & [\tilde{\tau}_1^i(s_1, \ldots, s_d) \; \ldots \; \tilde{\tau}_6^i(s_1, \ldots, s_d) \\ & \tilde{\lambda}_1^i(s_1, \ldots, s_d) \; \ldots \; \tilde{\lambda}_6^i(s_1, \ldots, s_d)] \end{aligned} \tag{2}$$

Matrix $\mathbf{Y}$ has $d(6+6)$ columns. Applying probabilistic principal component analysis (PPCA) (Tipping and Bishop, 1999) with m modes on $\mathbf{Y}$ results in a discrete linear model:

$$\begin{bmatrix} \tilde{\tau}_1(s_1 \ldots s_d)^T \\ \vdots \\ \tilde{\tau}_6(s_1 \ldots s_d)^T \\ \tilde{\lambda}_1(s_1 \ldots s_d)^T \\ \vdots \\ \tilde{\lambda}_6(s_1 \ldots s_d)^T \end{bmatrix} = \mathbf{H}\mathbf{x}^* + \mathbf{b} + \tilde{\boldsymbol{\varepsilon}} \tag{3}$$

with $p(\tilde{\boldsymbol{\varepsilon}}) = \mathcal{N}(\tilde{\boldsymbol{\varepsilon}} | \mathbf{0}, \sigma^2 \mathbf{I})$. Parameters $\mathbf{H}, \mathbf{b}$ and σ are found with an analytical formula: $\mathbf{b}$ is computed as the column mean of $\mathbf{Y}$ and $\mathbf{H}$ and σ are computed from an eigenvalue decomposition on the covariance of $\mathbf{Y}$ (Aertbeliën and De Schutter, 2014; Tipping and Bishop, 1999). Latent variables $\mathbf{x}^* \in \mathbb{R}^{m \times 1}$ do not have fixed values in the learning phase, but are described with a probability density function (Tipping and Bishop, 1999):

$$p(\mathbf{x}^*) = \mathcal{N}(\mathbf{x}^* | \mathbf{0}, \mathbf{I}) \tag{4}$$

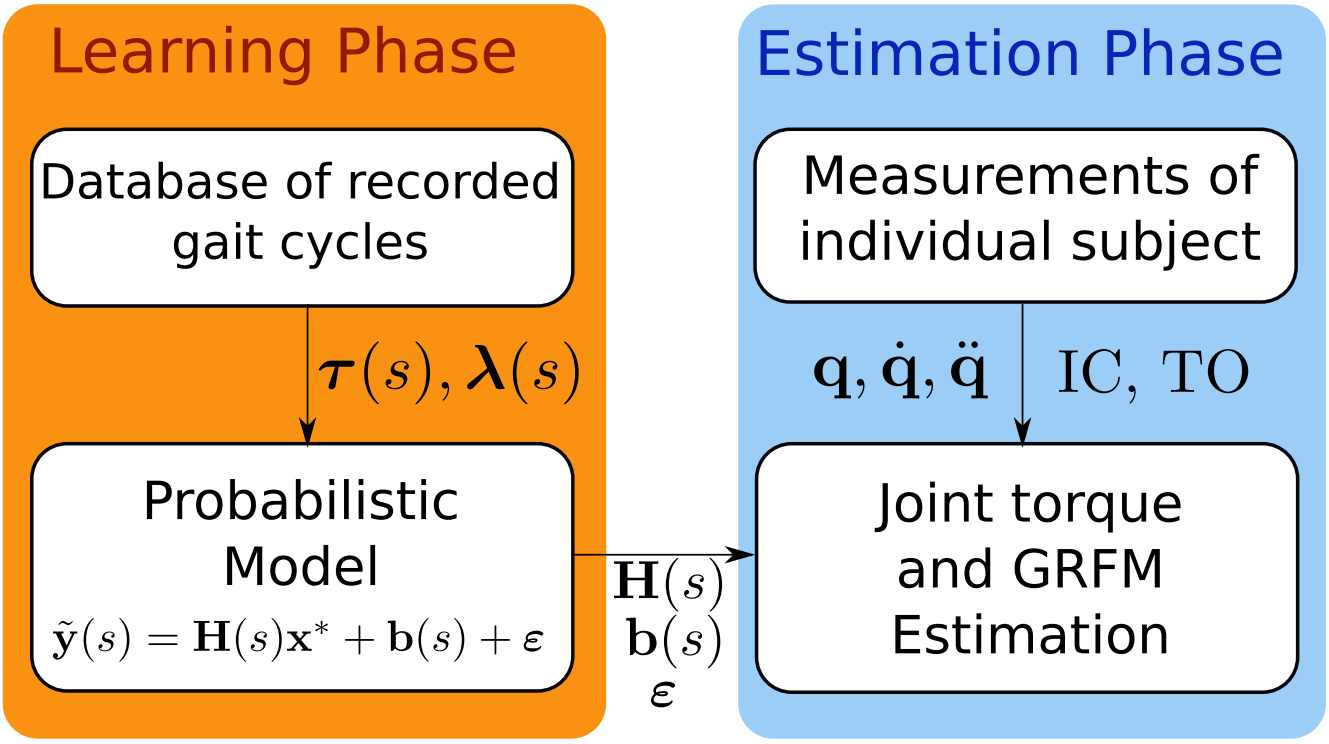

Fig. 1. Outline of the method. In the learning phase, see Section 2.2.1, the recorded GRFM $\boldsymbol{\lambda}$ and calculated joint torques $\boldsymbol{\tau}$ in function of normalized time s are used to learn the parameters $\mathbf{H}(s)$, $\mathbf{b}(s)$ and $\boldsymbol{\epsilon}$ of the probabilistic model $\tilde{\mathbf{y}}(s)$ describing the joint torques and GRFM scaled by body mass. In this phase, the latent variables $\mathbf{x}^*$ do not have a fixed value, but are characterized by a probability distribution. In the estimation phase, see 2.2.2, joint torques and GRFM are estimated to be as consistent as possible with the probabilistic model, the measurements of joint angles $\mathbf{q}$, velocities $\dot{\mathbf{q}}$ and accelerations $\ddot{\mathbf{q}}$ and the timing of initial contact (IC) and toe off (TO).

The number of latent variables should be chosen high enough to result in a good model, but not too high to avoid overfitting.

The discrete model (3) can be made continuous by applying piecewise linear interpolation (see Appendix A) resulting in

$$\tilde{\mathbf{y}}(s) = \begin{bmatrix} \tilde{\boldsymbol{\tau}}(s) \\ \tilde{\boldsymbol{\lambda}}(s) \end{bmatrix} = \mathbf{H}(s)\mathbf{x}^* + \mathbf{b}(s) + \tilde{\boldsymbol{\varepsilon}} \tag{5}$$

Vector $\mathbf{b}(s)$ can be interpreted as the expected value of $\tilde{\mathbf{y}}(s)$, while $\mathbf{H}(s)\mathbf{x}^*$ reflects the deviations from this expected value. The columns of matrix $\mathbf{H}(s)$ are basis functions describing the coupled deviations of joint torques and GRFM. The latent variables $\mathbf{x}^*$ are the coefficients corresponding to these basis functions. In this way a low number of discrete values $x_1^*, x_2^*, \ldots, x_m^*$ represents complete continuous trajectories of scaled joint torques and GRFM during the gait cycle.

2.2.2. Estimation phase

The learned model can be used to estimate the latent variables, the joint torques and GRFM of a new subject using only a skeletal model, kinematics and the timing of IC and TO as input. At each time instant, the dynamic equations of the lower limbs are written in function of s:

$$\mathbf{M}(\mathbf{q}(s))\ddot{\mathbf{q}}(\mathbf{s}) + \mathbf{h}(\mathbf{q}(s), \dot{\mathbf{q}}(\mathbf{s})) = \begin{bmatrix} \mathbf{0}_{6\times 1} \\ \boldsymbol{\tau}(s) \end{bmatrix} + \mathbf{J}_c(\mathbf{q}(s))^T \boldsymbol{\lambda}(s) \tag{6}$$

with $\mathbf{q}, \dot{\mathbf{q}}, \ddot{\mathbf{q}}$ the generalized angles, velocities and accelerations, $\mathbf{M}$ the mass matrix, $\mathbf{h}$ the Coriolis and gravity forces and $\mathbf{J}_c$ the contact Jacobian. The first six rows of Eq. (6) describe the motion of the floating base of the skeletal model (Featherstone, 2014), usually the pelvis, with respect to the world frame. These degrees of freedom are not actuated, leading to six zero elements in the joint torque vector.

Eq. (6) is written more compactly as:

$$\mathbf{z}(s) = \mathbf{A}(s)\mathbf{y}(s) \tag{7}$$

with

$$\mathbf{z}(s) = \mathbf{M}(\mathbf{q}(s))\ddot{\mathbf{q}}(\mathbf{s}) + \mathbf{h}(\mathbf{q}(s), \dot{\mathbf{q}}(\mathbf{s})) \tag{8}$$

$$\mathbf{A}(s) = \begin{bmatrix} \mathbf{0}_{6\times k} & \mathbf{J}_c(\mathbf{q}(s))^T \\ \mathbf{I}_{k\times k} & \end{bmatrix} \tag{9}$$

$$\mathbf{y}(s) = \mathbf{S}\tilde{\mathbf{y}}(s) = \mathbf{S}\begin{bmatrix} \tilde{\boldsymbol{\tau}}(s) \\ \tilde{\boldsymbol{\lambda}}(s) \end{bmatrix} \tag{10}$$

We used OpenSim (Delp et al., 2007) to calculate the values of $\mathbf{z}$ and $\mathbf{A}$ from the measured kinematics and a skeletal model of the subject. The value of s is determined from the measurements of IC.

The a posteriori probability distribution of the joint torques and GRFM is equal to (see Appendix B):

$$p(\mathbf{y}|\mathbf{z}(s), s) = \mathcal{N}(\mathbf{y}|\boldsymbol{\mu}_2, \boldsymbol{\Sigma}_2) \tag{11}$$

with $\boldsymbol{\Sigma}_2 = \mathbf{S}\mathbf{H}(s)\boldsymbol{\Sigma}_1\mathbf{H}(s)^T\mathbf{S}^T + \sigma^2\mathbf{S}\mathbf{S}^T, \boldsymbol{\Sigma}_1 = \left(\mathbf{I} + \mathbf{B}^T\mathbf{D}^{-1}\mathbf{B}\right)^{-1}$, $\boldsymbol{\mu}_2 = \mathbf{S}\left(\mathbf{H}(s)\boldsymbol{\mu}_1 + \mathbf{b}(s)\right)$ and $\boldsymbol{\mu}_1 = \boldsymbol{\Sigma}_1\mathbf{B}^T\mathbf{D}^{-1}(\mathbf{z} - \mathbf{c})$. The most probable values of the joint torques and GRFM that satisfy the dynamic equations are found by solving a convex quadratic optimization program:

$$\begin{aligned} \min_{\mathbf{y}} \quad & \tfrac{1}{2}(\mathbf{y} - \boldsymbol{\mu}_2)^T\boldsymbol{\Sigma}_2^{-1}(\mathbf{y} - \boldsymbol{\mu}_2) \\ \text{s.t.} \quad & \mathbf{z}_p(s) = \mathbf{A}_p(s)\mathbf{y} \end{aligned} \tag{12}$$

where index p indicates the subset of dynamic equations without the equations for the floating base. The dynamic equations for the floating base do not have to be satisfied exactly, since inaccuracies

in estimated body segment parameters and kinematics result in dynamic inconsistency (Fluit et al., 2014). When a leg is in swing phase, which is determined from the measured IC and TO timing, extra constraints are added to Eq. (12) to set the GRFM acting on this leg equal to zero. This calculation is done for every time instant in the Matlab scripting language.

2.3. Validation

The method was validated in three ways. Firstly, we used cross-validation by splitting up the total dataset into a validation set containing all recordings of one subject and a learning set containing recordings of all other subjects. Hence, the learned probabilistic model had no information on the validation subject. The estimated GRFM and joint torques were compared to their ground truth values, which are, respectively, the measured GRFM and the joint torques resulting from inverse dynamics with measured GRFM. We repeated this until each subject was used for validation and excluded for learning once.

Secondly, we investigated how the method performed in new conditions. We estimated the joint torques and GRFM of the 5 km/h walking trial of a subject using only the 3 and 4 km/h walking trials of the other subjects during learning. Hence, the method had never seen data of the subject, nor had it observed walking at 5 km/h. This was again repeated for all subjects.

Finally, we compared our method with different state-of-the-art methods: (i) the Smooth Transition Assumption (STA) method (Ren et al., 2008), (ii) the Zero Moment Point (ZMP) method (Dijkstra and Gutierrez-Farewik, 2015), (iii) the optimization (Opt) method (Fluit et al., 2014) and (iv) the Artificial Neural Network (ANN) method (Oh et al., 2013), which were briefly described in the introduction.

3. Results

Using cross-validation, the best results were found with $m = 4$ latent variables. Fig. 2 shows the estimated and ground truth values of the joint torques and GRFM for two gait cycles at 5 km/h of a representative subject. Table 1 shows the statistics of the estimation error for the complete validation over all subjects: the mean error, the standard deviation (std), the maximum absolute error, the root mean square error relative to the body mass RMSE_m and relative to the range of the signal RMSE_r and the mean of the peak-to-peak error mean_{p2p}, computed as the difference between the maximal estimation value and the maximal ground truth value for each gait cycle, relative to the signal range. The vertical force had the largest RMSE_m due to its steep curve during double support. However, relative to its range it was the best estimated GRFM component with a value of 3.6%. The RMSE for the estimated joint torques were approximately 0.1 Nm/kg, which is between 6 and 18 % of the range of the signal. The estimation was unbiased, as the mean error was almost equal to zero. Sometimes, the maximum absolute value of the error was quite large. However, the probability of getting such a large error was smaller than 1% as these maximum values were larger than three times the standard deviation. The mean peak-to-peak error is zero except for the hip rotation torque.

Fig. 3 shows the estimation results for the same trial as in Fig. 2, but now with a learning dataset containing only trials from 3 and 4 km/h. Overall, the estimation was slightly worse than with a complete learning set, see Table 2. The vertical GRF, anterior-posterior GRF, hip flexion and knee flexion estimation were no longer unbiased. The standard deviation and RMSE_m of all estimated signals were higher than in the case with a complete learning set. However, the RMSE_r errors of the joint torques did not change a lot. This means that the joint torque estimation error was higher in absolute terms, but remained constant relative to the range of the joint torques, which had increased due to the increased speed. On average, the peak values were underestimated.

Table 3 compares our results with reported results from state-of-the-art methods. Our method outperformed the state of the art in many cases. All sagittal plane GRFM and joint torques of the STA method had a larger error compared to our method. For example, the hip and knee flexion error of the STA method were three times larger. This is probably because the STA method uses only a priori information of the GRFM, whereas our method also uses knowledge of the joint torques. The ZMP and Opt methods also performed worse than our method. The error difference was the largest for the vertical and anterior-posterior GRFM. For the ANN method, the estimation error of the vertical GRF was about 1.6 times bigger than our estimation error. However, all other components were predicted better with the ANN method. The estimation errors for the ankle torque were only slightly better, but hip joint torques errors were three times smaller and knee flexion errors are about five times smaller.

The computational load of our method is low, since it only requires small matrix operations and solving a small quadratic equality constrained problem. Learning a model for one subject, using the gait data of 22 other subjects on average took 0.7 s. Estimating the torques and GRFM on average took 0.28 ms per time instant, of which 0.1 ms was needed for the calculation of the terms $\mathbf{M}(\mathbf{q}), \mathbf{h}(\mathbf{q}, \dot{\mathbf{q}})$ and $\mathbf{J}_c(\mathbf{q})$ of Eq. (6).

4. Discussion

The estimated curves were very similar to the ground truth, see Fig. 2. The peak values of the hip flexion torque and anterior-posterior GRF were slightly underestimated. However, on average our method only underestimated the peak value of the hip rotation torque, as shown in the last column of Table 1. When the trials at 5 km/h were removed from the learning set, peak values were on average underestimated since higher walking speeds resulted in higher joint torques and GRFM than observed in the dataset.

During validation, the learning dataset contained data of 22 subjects. However, a good model can also be learned with less training data: lowering the number of subjects in the learning dataset to 5 increased the RMSE_m values with only 5%.

As mentioned above, the joint torques and GRFM during single support can be estimated by solving the dynamic equations of lower limbs and pelvis. This solution is however a lot more sensitive to inaccuracies in the skeletal model than our solution, leading to increased RMSE_m values of 40% for the ankle torque, 25% for knee flexion and adduction torque and 15% for hip flexion torque.

When comparing our results to reported state-of-the-art results, we note that subjects walked on a treadmill in our study, whereas subjects walked overground in the other studies. Due to treadmill vibrations, the measured GRFM contain more noise, leading to larger dynamic inconsistency which makes estimation harder. Nevertheless, our method clearly outperformed STA, ZMP and Opt methods. The ANN method displayed lower errors than our method in most cases, but our method has some advantages over the ANN method. Firstly, the parameter estimation of our method is not sensitive to an initial guess, which makes it more repeatable. Furthermore, ANN is a black-box high-dimensional fit whereas our method uses a model with insight into the physical properties of the system. This makes it possible to predict if the method is still applicable in new situations: one can verify that the mean value $\mathbf{b}(s)$ is still a good approximation of the measured value and that the measured deviations from the mean can be established with the learned basis functions $\mathbf{H}(s)$. With ANN, the

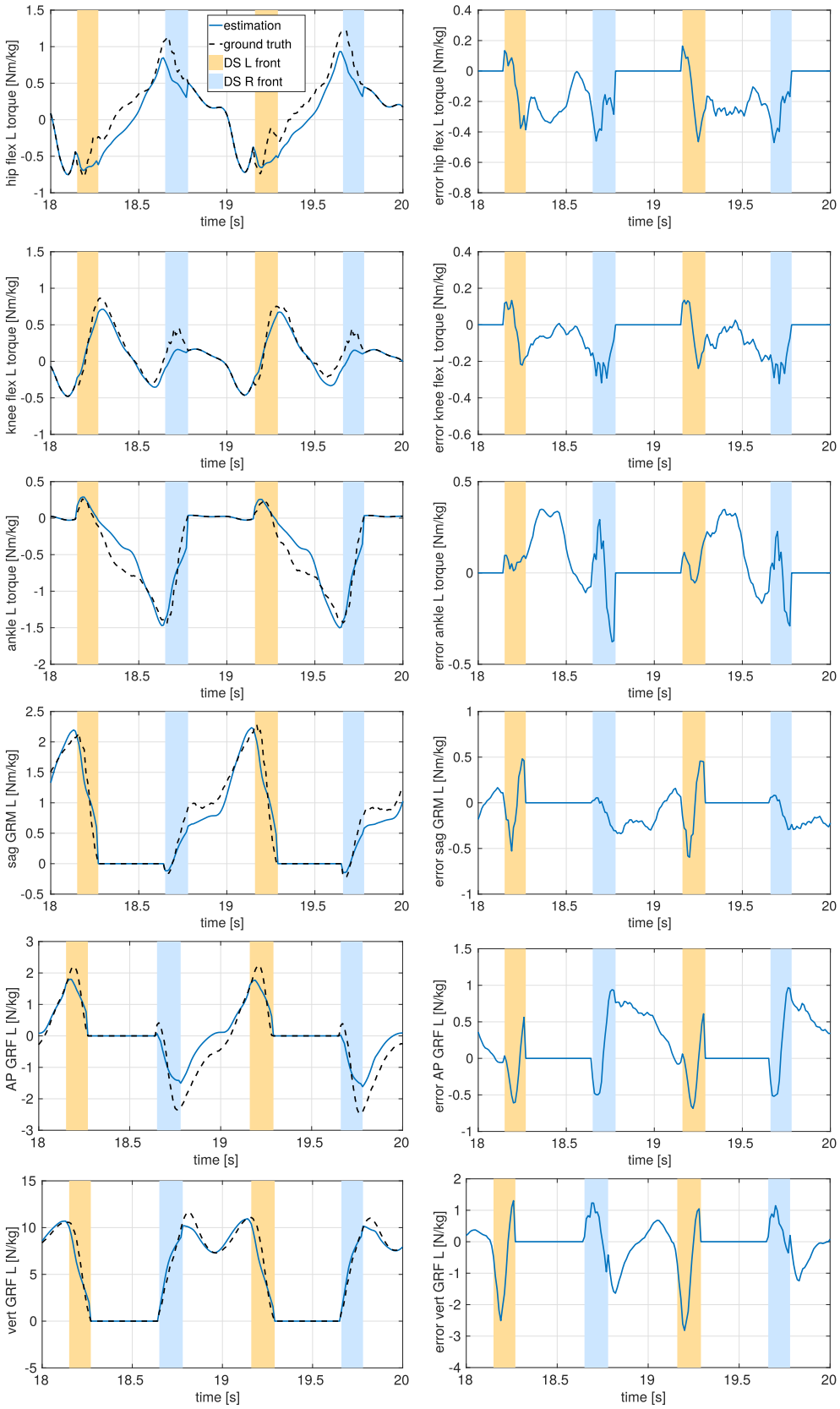

Fig. 2. Estimation of two consecutive gait cycles at 5 km/h using the full learning set. The left columns show the sagittal hip flexion, knee flexion and ankle torque of the left leg and the sagittal moment, the anterior-posterior force and the vertical force on the left calcaneus. The estimated values are shown in blue, the reference values are in black. Areas with orange and blue background are, respectively, double support periods with the left and right leg in front. The right columns shows the difference between reference and estimation.

Table 1
Estimation errors of the vertical, anterior-posterior and medio-lateral ground reaction force, the sagittal, frontal and transverse ground reaction moment and the joint torques. The columns for mean, standard deviation, absolute maximum and root mean square error relative to body mass $RMSE_m$ are expressend in N/kg or Nm/kg. The root mean square error relative to the range of the signal $RMSE_r$ and the mean peak-to-peak error $mean_{p2p}$ relative to the range of the signal are dimensionless.

	mean	std	|max|	$RMSE_m$	$RMSE_r$	$mean_{p2p}$
Vert GRF	−0.053	0.407	3.159	0.411	0.036	−0.009
AP GRF	0.006	0.191	1.271	0.192	0.051	−0.040
ML GRF	0.059	0.158	0.982	0.169	0.117	−0.011
Sag GRM	−0.006	0.126	0.929	0.126	0.056	0.021
Front GRM	0.002	0.092	0.690	0.092	0.180	0.102
Transv GRM	−0.031	0.077	0.690	0.083	0.213	−0.066
hip flex torque	0.005	0.138	0.971	0.138	0.096	−0.041
hip add torque	0.015	0.135	0.768	0.136	0.121	−0.033
hip rot torque	0.009	0.077	0.584	0.077	0.183	−0.167
knee flex torque	0.003	0.104	0.756	0.104	0.091	−0.030
knee add torque	0.007	0.086	0.596	0.086	0.153	−0.024
ankle flex torque	0.005	0.118	0.837	0.118	0.065	0.024

validity of the learned model cannot be predicted for new situations. Finally, our method is probabilistic, also yielding information about the uncertainty of the estimates.

A limitation of this study is that the gait event inputs were determined from force plate data which is not available in the intended applications for our method. However, foot switches can be used to accurately determine the timing of these events, with a mean difference of 0 ± 3 ms for IC and -1 ± 8 ms for TO (Hausdorff et al., 1995). Perturbing the timing of IC and TO in simulation with these mean and standard deviation values increased the $RMSE_m$ values only with 0–4%.

In our methodology, we learned a generic probabilistic model for the joint torques and GRFM, applicable for all healthy subjects. It is however also possible to learn a subject-specific model by only using training data from experiments of a specific subject. This subject-specific model can then be used to estimate joint torques and GRFM of this subject in situations where it is not possible to measure GRFM. Evidently, a subject-specific model will result in lower estimation errors than a generic model.

In future work, this method can potentially be used for impaired subjects if a training dataset, representative for the pathology of the subject, is available. Having a representative dataset will be easier for musculoskeletal disorders, such as osteoarthrosis, than for neurological disorders. The method could also be integrated in computationally demanding problems such as forward gait simulations, which now often rely on foot-ground contact models resulting in stiff skeletal dynamics with high computational load. Replacing the contact model with our model could reduce the computational load and hence also calculation time. The method could also be used for realtime applications, for instance for realtime feedback during rehabilitation or for use in wearable devices such as exoskeletons. Our current method needs to know the timing of the future IC and TO events to determine the value of s, but this can possibly be derived from the timing of the events of the previous step.

5. Conclusion

In this work, a probabilistic method was presented to estimate joint torques and GRFM during gait using only a skeletal model, measured kinematics and timing of IC and TO as input. The method outperforms model-based state-of-the-art methods. Compared to model-free neural networks the method is only better for the vertical reaction force component, but it has the advantage of better repeatability, uncertainty information on the estimate and the possibility to verify the applicability of the method in new situations. We showed that we are still able to estimate joint torques and GRFM at walking speeds higher than in the learning dataset.

Declaration of Competing Interest

The authors declare that they do not have a conflict of interest.

Acknowledgment

This project was funded by the Flemish agency for Innovation by Science and Technology through a project grant (MIRAD, IWT-SBO 120057).

Appendix A. From discrete to continuous probabilistic model

To obtain a continuous model, we first focus on the values of the first joint torque during a gait cycle, i.e. the first d rows of Eq. (3):

$$\begin{bmatrix} \tilde{\tau}_{1,s_1} \\ \tilde{\tau}_{1,s_2} \\ \vdots \\ \tilde{\tau}_{1,s_d} \end{bmatrix} = \mathbf{H}_{\tau_1}\mathbf{x}^* + \mathbf{b}_{\tau_1} + \boldsymbol{\varepsilon}_{\tau_1} = \begin{bmatrix} h_{1,s_1} & h_{2,s_1} & \dots & h_{m,s_1} \\ h_{1,s_2} & h_{2,s_2} & \dots & h_{m,s_2} \\ \vdots & \vdots & \ddots & \vdots \\ h_{1,s_d} & h_{2,s_d} & \dots & h_{m,s_d} \end{bmatrix} \mathbf{x}^* + \begin{bmatrix} b_{s_1} \\ b_{s_2} \\ \vdots \\ b_{s_d} \end{bmatrix} + \boldsymbol{\varepsilon}_{\tau_1} \quad (A.1)$$

We then interpolate the columns of $\mathbf{H}_{\tau_1}$ and $\mathbf{b}_{\tau_1}$ and obtain a continuous model for the first scaled joint torque:

$$\tilde{\tau}_1(s) = [\, h_1(s) \quad h_2(s) \quad \dots \quad h_m(s) \,]\mathbf{x}^* + b(s) + \varepsilon(s) \quad (A.2)$$

with $\varepsilon(s) \sim \mathcal{N}(0, \sigma^2)\ \forall s$. The used interpolation function is up to the choice of the user. In this research, piecewise linear interpolation functions are used.

The above technique can be repeated for the other scaled joint torques and GRFM components:

$$\begin{bmatrix} \tilde{\tau}_1(s) \\ \vdots \\ \tilde{\tau}_6(s) \\ \tilde{\lambda}_1(s) \\ \vdots \\ \tilde{\lambda}_6(s) \end{bmatrix} = \begin{bmatrix} \mathbf{H}_{\tilde{\tau}_1}(s) \\ \vdots \\ \mathbf{H}_{\tilde{\tau}_6}(s) \\ \mathbf{H}_{\tilde{\lambda}_1}(s) \\ \vdots \\ \mathbf{H}_{\tilde{\lambda}_6}(s) \end{bmatrix} \mathbf{x}^* + \begin{bmatrix} \mathbf{b}_{\tilde{\tau}_1}(s) \\ \vdots \\ \mathbf{b}_{\tilde{\tau}_6}(s) \\ \mathbf{b}_{\tilde{\lambda}_1}(s) \\ \vdots \\ \mathbf{b}_{\tilde{\lambda}_6}(s) \end{bmatrix} + \tilde{\boldsymbol{\varepsilon}} \quad (A.3)$$

which is written more compactly as

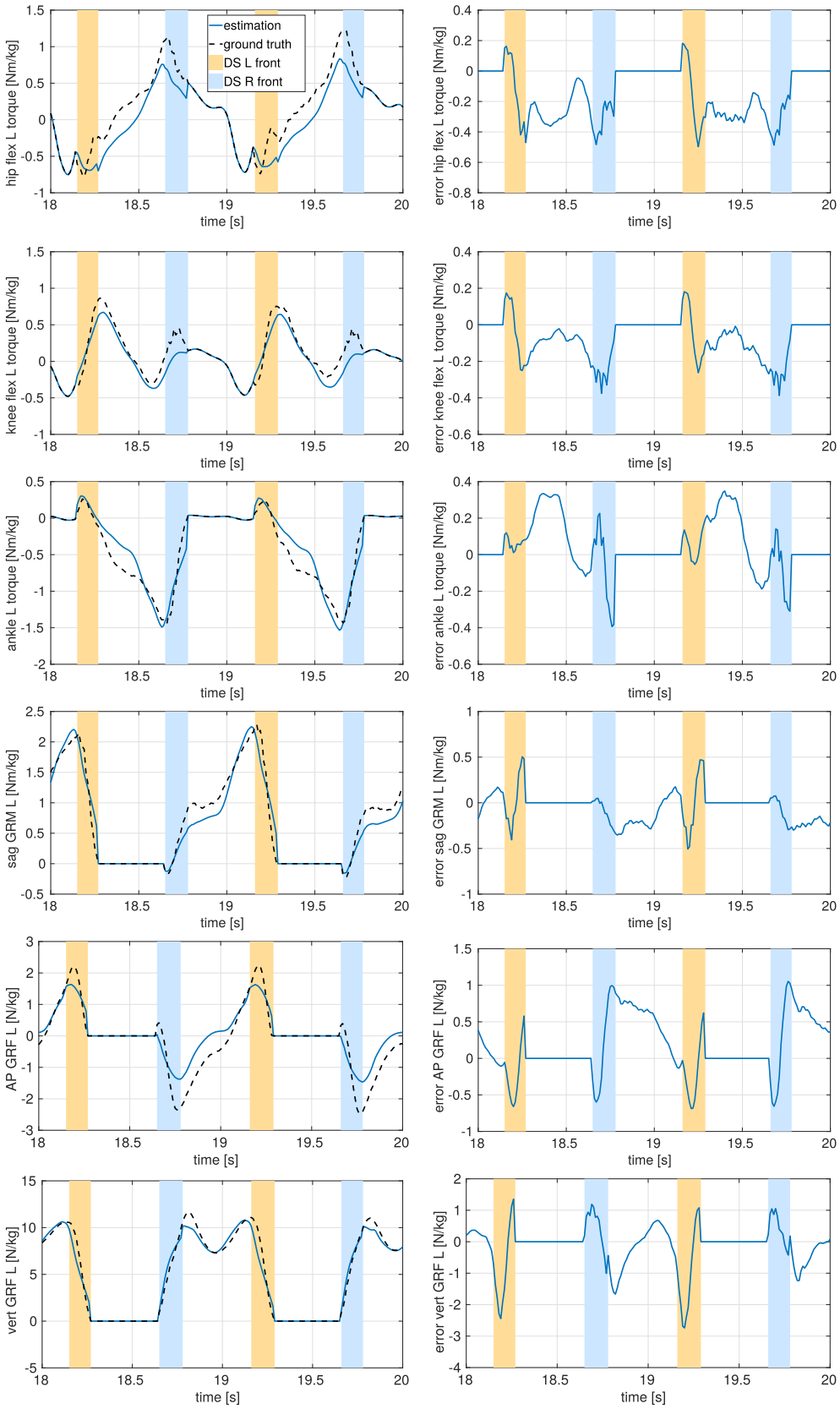

Fig. 3. Estimation of two consecutive gait cycles at 5 km/h using learning data of 3 and 4 km/h. The left columns show the sagittal hip flexion, knee flexion and ankle torque of the left leg and the sagittal moment, the anteriorposterior force and the vertical force on the left calcaneus. The estimated values are shown in blue, the reference values are in black. Areas with orange and blue background are, respectively, double support periods with the left and right leg in front. The right columns shows the difference between reference and estimation.

Table 2
Statistics of the estimation errors for trials at 5 km/h resulting from a learning dataset with only trials between 3 and 4 km/h.

	mean	std	|max|	$RMSE_m$	$RMSE_r$	$mean_{p2p}$
Vert GRF	−0.204	0.636	3.036	0.668	0.055	−0.062
AP GRF	0.139	0.371	1.451	0.397	0.077	−0.139
ML GRF	0.009	0.219	0.967	0.219	0.116	−0.142
Sag GRM	−0.025	0.199	0.906	0.201	0.078	0.024
Front GRM	0.045	0.137	0.685	0.144	0.198	−0.031
Transv GRM	0.006	0.123	0.707	0.123	0.180	0.029
hip flex torque	−0.127	0.219	1.080	0.253	0.117	−0.142
hip add torque	0.038	0.195	0.773	0.199	0.123	−0.160
hip rot torque	−0.016	0.123	0.644	0.124	0.184	−0.111
knee flex torque	−0.071	0.177	0.828	0.191	0.122	−0.159
knee add torque	0.008	0.132	0.617	0.132	0.160	−0.119
ankle flex torque	0.019	0.185	0.798	0.186	0.089	0.030

Table 3
Comparison of the $RMSE_m$ values of the estimated joint torques and GRFM over a complete gait cycle in N/kg or Nm/kg for different methods: the Smooth Transition Assumption (STA) (Ren et al., 2008), Zero Moment Point method (ZMP) (Dijkstra and Gutierrez-Farewik, 2015), the Optimization method (Opt) (Fluit et al., 2014), the Artificial Neural Network (ANN) (Oh et al., 2013) and our method (PPCA). Not all results are reported (NR) in the cited works.

	STA	ZMP	Opt	ANN	PPCA
participants	3	10	9	48	23
condition	overground	overground	overground	overground	treadmill
speed	5.4 km/h	self-selected	self-selected	self-selected	3–5 km/h
Vert GRF	0.710	0.900	0.740	0.649	0.411
AP GRF	0.473	0.520	0.380	0.154	0.192
ML GRF	0.191	0.150	0.170	0.040	0.169
Sag GRM	0.199	NR	0.180	0.081	0.126
Front GRM	0.148	NR	0.110	0.052	0.092
Transv GRM	0.039	NR	0.220	0.032	0.083
hip flex torque	0.469	NR	NR	0.056	0.138
hip add torque	0.106	NR	NR	0.052	0.136
hip rot torque	0.051	NR	NR	0.029	0.077
knee flex torque	0.307	NR	NR	0.020	0.104
knee add torque	0.100	NR	NR	0.033	0.086
ankle flex torque	0.190	NR	NR	0.091	0.118

$$\tilde{\mathbf{y}}(s) = \begin{bmatrix} \tilde{\boldsymbol{\tau}}(s) \\ \tilde{\boldsymbol{\lambda}}(s) \end{bmatrix} = \mathbf{H}(s)\mathbf{x}^* + \mathbf{b}(s) + \tilde{\boldsymbol{\varepsilon}} \tag{A.4}$$

with $\mathbf{H}(s)$ is a $(6+6) \times m$ matrix and $\mathbf{b}(s)$ is a $(6+6) \times 1$ vector of interpolation functions. In this way a low number of discrete values $x_1^*, x_2^*, \ldots, x_m^*$ represents complete continuous trajectories of scaled joint torques and GRFM during the gait cycle.

Appendix B. A posteriori distribution of scaled variables

Given the measurements $\mathbf{z}$ and s from Eq. (7), the joint torques and GRFM can be estimated using the formulas for conditional and marginal Gaussian distributions (Bishop, 2006). From Eq. (5), we can see that the probability distribution of $\tilde{\mathbf{y}}$, given values of $\mathbf{x}^*$ and s is normally distributed:

$$p(\tilde{\mathbf{y}}|\mathbf{x}^*, s) = \mathcal{N}(\tilde{\mathbf{y}}|\mathbf{H}(s)\mathbf{x}^* + \mathbf{b}(s), \sigma^2\mathbf{I}) \tag{B.1}$$

Using Eqs. (7) and (10), we can derive that $\mathbf{z}$ is also normally distributed:

$$p(\mathbf{z}|\mathbf{x}^*, s) = \mathcal{N}(\mathbf{z}|\mathbf{B}\mathbf{x}^* + \mathbf{c}, \mathbf{D}) \tag{B.2}$$

with $\mathbf{B} = \mathbf{A}\mathbf{S}\mathbf{H}(s)$, $\mathbf{c} = \mathbf{A}\mathbf{S}\mathbf{b}(s)$ and $\mathbf{D} = \sigma^2\mathbf{A}\mathbf{S}\mathbf{S}^T\mathbf{A}^T$. The a posteriori distribution of the latent variables can be computed from Eqs. (4) and (B.2):

$$p(\mathbf{x}^*|\mathbf{z}(s), s) = \mathcal{N}(\mathbf{x}^*|\boldsymbol{\mu}_1, \boldsymbol{\Sigma}_1) \tag{B.3}$$

with $\boldsymbol{\Sigma}_1 = \left(\mathbf{I} + \mathbf{B}^T\mathbf{D}^{-1}\mathbf{B}\right)^{-1}$ and $\boldsymbol{\mu}_1 = \boldsymbol{\Sigma}_1\mathbf{B}^T\mathbf{D}^{-1}(\mathbf{z} - \mathbf{c})$. Using Eqs. (5) and (10) results in the probability distribution of the joint torques and GRFM given the measurements $\mathbf{z}$ and s:

$$p(\mathbf{y}|\mathbf{z}(s), s) = \mathcal{N}(\mathbf{y}|\boldsymbol{\mu}_2, \boldsymbol{\Sigma}_2) \tag{B.4}$$

with $\boldsymbol{\Sigma}_2 = \mathbf{S}\mathbf{H}(s)\boldsymbol{\Sigma}_1\mathbf{H}(s)^T\mathbf{S}^T + \sigma^2\mathbf{S}\mathbf{S}^T$ and $\boldsymbol{\mu}_2 = \mathbf{S}\big(\mathbf{H}(s)\boldsymbol{\mu}_1 + \mathbf{b}(s)\big)$.

Appendix C. Supplementary material

Supplementary data associated with this article can be found, in the online version, at https://doi.org/10.1016/j.jbiomech.2019.109327.

References

Aertbeliën, E., De Schutter, J., 2014. Learning a predictive model of human gait for the control of a lower-limb exoskeleton. In: 5th IEEE RAS/EMBS International Conference on Biomedical Robotics and Biomechatronics. IEEE, pp. 520–525.

Bishop, C.M., 2006. Pattern Recognition and Machine Learning. Springer, pp. 91–93 (Chapter 2).

Chambers, H.G., Sutherland, D.H., 2002. A practical guide to gait analysis. JAAOS-J. Am. Acad. Orthop. Surg. 10, 222–231.

Chumanov, E.S., Remy, C.D., Thelen, D.G., 2010. Computational techniques for using insole pressure sensors to analyse three-dimensional joint kinetics. Comput. Methods Biomech. Biomed. Eng. 13, 505–514.

Davis, B.L., Cavanagh, P.R., 1993. Decomposition of superimposed ground reaction forces into left and right force profiles. J. Biomech. 26, 593–597.

Davis III, R.B., Ounpuu, S., Tyburski, D., Gage, J.R., 1991. A gait analysis data collection and reduction technique. Hum. Movement Sci. 10, 575–587.

De Groote, F., De Laet, T., Jonkers, I., De Schutter, J., 2008. Kalman smoothing improves the estimation of joint kinematics and kinetics in marker-based human gait analysis. J. Biomech. 41, 3390–3398.

Delp, S.L., Anderson, F.C., Arnold, A.S., Loan, P., Habib, A., John, C.T., Guendelman, E., Thelen, D.G., 2007. Opensim: open-source software to create and analyze dynamic simulations of movement. IEEE Trans. Biomed. Eng. 54, 1940–1950.

Dijkstra, E.J., Gutierrez-Farewik, E.M., 2015. Computation of ground reaction force using zero moment point. J. Biomech. 48, 3776–3781.

Featherstone, R., 2014. Rigid Body Dynamics Algorithms. Springer.

Fluit, R., Andersen, M.S., Kolk, S., Verdonschot, N., Koopman, H.F., 2014. Prediction of ground reaction forces and moments during various activities of daily living. J. Biomech. 47, 2321–2329.
Gage, J.R., 1993. Gait analysis. an essential tool in the treatment of cerebral palsy. Clin. Orthop. Related Res., 126–134
Hamner, S.R., Seth, A., Delp, S.L., 2010. Muscle contributions to propulsion and support during running. J. Biomech. 43, 2709–2716.
Hausdorff, J.M., Ladin, Z., Wei, J.Y., 1995. Footswitch system for measurement of the temporal parameters of gait. J. Biomech. 28, 347–351.
Jackson, J.N., Hass, C.J., Fregly, B.J., 2016. Development of a subject-specific foot-ground contact model for walking. J. Biomech. Eng. 138, 091002.
Jung, Y., Jung, M., Lee, K., Koo, S., 2014. Ground reaction force estimation using an insole-type pressure mat and joint kinematics during walking. J. Biomech. 47, 2693–2699.
Khurelbaatar, T., Kim, K., Lee, S., Kim, Y.H., 2015. Consistent accuracy in whole-body joint kinetics during gait using wearable inertial motion sensors and in-shoe pressure sensors. Gait Posture 42, 65–69.
Lugrís, U., Carlín, J., Pàmies-Vilà, R., Font-Llagunes, J.M., Cuadrado, J., 2013. Solution methods for the double-support indeterminacy in human gait. Multibody Syst. Dyn. 30, 247–263.
Oh, S.E., Choi, A., Mun, J.H., 2013. Prediction of ground reaction forces during gait based on kinematics and a neural network model. J. Biomech. 46, 2372–2380.
OpenSim, 2009. Public available musculoskeletal model https://simtk-confluence.stanford.edu/display/OpenSim/Full+Body+Running+Model (accessed December 3, 2018).
Ren, L., Jones, R.K., Howard, D., 2008. Whole body inverse dynamics over a complete gait cycle based only on measured kinematics. J. Biomech. 41, 2750–2759.
Samadi, B., Raison, M., Ballaz, L., Achiche, S., 2017. Decomposition of three-dimensional ground-reaction forces under both feet during gait. J. Musculoskelet. Neuronal Interact. 17, 283.
Schepers, H.M., Koopman, H.F., Veltink, P.H., 2007. Ambulatory assessment of ankle and foot dynamics. IEEE Trans. Biomed. Eng. 54, 895–902.
Shahabpoor, E., Pavic, A., 2018. Estimation of tri-axial walking ground reaction forces of left and right foot from total forces in real-life environments. Sensors 18.
Simon, S.R., 2004. Quantification of human motion: gait analysis-benefits and limitations to its application to clinical problems. J. Biomech. 37, 1869–1880.
Tipping, M.E., Bishop, C.M., 1999. Probabilistic principal component analysis. J. Roy. Stat. Soc. Ser. B (Stat. Methodol.) 61, 611–622.
Winter, D.A., 1987. The Biomechanics and Motor Control of Human Gait. University of Waterloo Press.
Zheng, R., Liu, T., Inoue, Y., Shibata, K., Liu, K., 2008. Kinetics analysis of ankle, knee and hip joints using a wearable sensor system. J. Biomech. Sci. Eng. 3, 343–355.